

**TASEP modelling provides a parsimonious explanation for the ability of a single
uORF to derepress translation during the Integrated Stress Response.**

by

*Dmitry E Andreev^{1,2†}, Maxim Arnold^{3†}, Stephen J. Kiniry¹, Gary Loughran¹, Audrey Michel¹,
Dmitrii Rachinskiy^{3*}, Pavel V Baranov^{1*}.*

¹ School of Biochemistry and Cell Biology, University College Cork, Ireland

² Belozersky Institute of Physico-Chemical Biology, Lomonosov Moscow State University, Russia

³ Department of Mathematical Sciences, The University of Texas at Dallas, USA

† These authors contributed equally to this work

* Correspondent author: p.baranov@ucc.ie; dmitry.rachinskiy@utdallas.edu

ABSTRACT

Translation initiation is the rate-limiting step of protein synthesis that is downregulated during the Integrated Stress Response (ISR). Previously we demonstrated that most human mRNAs resistant to this inhibition possess translated uORFs, and that in some cases a single uORF is sufficient for the resistance (Andreev et al., 2015). Here we developed a computational model of Initiation Complexes Interference with Elongating Ribosomes (ICIER) to gain insight into the mechanism. We explored the relationship between the flux of scanning ribosomes upstream and downstream of a single uORF depending on uORF features. Paradoxically our analysis predicts that reducing ribosome flux upstream of certain uORFs increases initiation downstream. The model supports the derepression of downstream translation as a general mechanism of uORF-mediated stress resistance. It predicts that stress resistance can be achieved with long slowly decoded uORFs that do not favor translation reinitiation and start with initiators of low leakiness.

INTRODUCTION

In eukaryotes, canonical translation initiation begins with the recognition of the m7G cap structure found at the 5' end of mRNAs. This is achieved by the multi-subunit eIF4F complex consisting of a cap-binding subunit, eIF4E, a helicase eIF4A and a scaffold protein eIF4G. eIF4F then recruits the 40S loaded with eIF2*tRNA*GTP (so called ternary complex, TC), eIF1, eIF1A and eIF5, along with multi-subunit scaffold eIF3 forming a preinitiation complex (PIC). Then the PIC starts to "scan" the mRNA, unwinding mRNA secondary structures and probing mRNA for potential sites of translation initiation. After the initiation codon is recognized, the chain of events leads to large ribosome subunit joining and initiation of polypeptide synthesis. For more details see recent reviews (1-5) on the mechanism of translation initiation in eukaryotes and its regulation.

Not all translation initiation events lead to the synthesis of annotated functional proteins. Many codons recognized as starts of translation occur upstream of annotated coding ORFs (acORFs) encoding functional proteins in many eukaryotic organisms (6-12). Leader length varies greatly in mammalian mRNAs and at least 20% possess evolutionarily conserved AUG triplets upstream of acORFs (13). The number of potential sites of translation initiation is even higher due to initiation at near-cognate non-AUG codons (most frequently CUG) (14-17). This is particularly prevalent for non-AUG codons located upstream of the first AUG codon, since they are the first to be encountered by the PIC (18). Abundant translation initiation upstream of acORFs has been confirmed by several ribosome profiling experiments (19-21). Ribosome profiling also revealed that the translation of these ORFs is often altered in response to changes in physiological conditions. A number of stress conditions lead to a global increase in translation of mRNA leaders (22-25). Sometimes reciprocal changes in acORF translation can be observed among individual mRNAs (22). One of the stress conditions where uORF-mediated translation control seems to be particularly important is in the ISR (26-28). The ISR induces the phosphorylation of the alpha subunit of eIF2 by one of several stress-sensing kinases. This leads to the inhibition of its recycling to eIF2*tRNA*GTP carried out by recycling factor eIF2B and to global repression of protein synthesis (29). We and others recently showed that the translation of a small number of mRNAs are resistant or upregulated during ISR, and the most stress resistant mRNAs possess translated uORFs (26,30).

The classical mechanism of uORF mediated stress resistance, known as delayed reinitiation, occurs in *GCN4* mRNA, the archetypical example of this mechanism in yeast (reviewed in (31)). Although *GCN4* regulation involves several uORFs (32-34), only two are absolutely essential for stress resistance. After translation termination at a short uORF located close to the 5' end, the 40S resumes scanning albeit without the TC. The distance scanned by this ribosome subunit before the ribosome reacquires the TC depends on TC availability. Under normal conditions most of the 40S is quickly reloaded with TC and therefore can reinitiate at a downstream inhibitory uORF. Ribosomes translating this second uORF cannot reinitiate at the acORF start. Under low eIF2 availability, a larger fraction of 40S subunits bypass the second uORF initiation codon before binding of the TC, thereby enabling acORF translation. However, examples, have been found where only a single uORF is sufficient for providing a mRNA with translational stress resistance, e. g. *DDIT3* (35,36), *PPP1R15A* (37), *ZFAND2A* (38), *IFRD1* and *PPP1R15B* (26).

The start codon of the *DDIT3* uORF is in a suboptimal Kozak context and allows for leaky scanning (35,39). However, the uORF encodes a specific peptide sequence that stalls ribosomes under normal conditions creating a barrier for trailing PICs which results in strong inhibition of downstream translation (39). It has been hypothesized that the stringency of start codon recognition is increased during particular stress conditions and this allows for more leaky scanning (35,39).

It is also possible that elongating ribosomes translating the uORF obstruct progression of scanning ribosomes downstream and this obstruction is relieved during stress due to reduced initiation

at the uORF. Although the obstruction of scanning ribosomes may potentially explain how a single uORF can mediate stress resistance, it is unclear whether such a mechanism is plausible without additional factors involved. While most stress resistant mRNAs possess uORFs, only very few uORF-containing mRNAs are stress resistant (26). What makes some uORFs to be the providers of stress resistance? To explore this, we developed a simple stochastic model of Initiation Complexes Interference with Elongating Ribosomes (ICIER) that is based on the Totally Asymmetric Simple Exclusion Process (TASEP). TASEP is a dynamic system of unidirectional particle movement through a one-dimensional lattice, where each site can be occupied by no more than one particle and the probability of particle transition from one site to another is predefined. TASEP is widely used for modelling various dynamic systems, such as road traffic and is also popular in modelling mRNA translation (40-45). In ICIER we represent scanning and elongating ribosomes as two separate types of particles with different dynamic properties with the possibility of transformation of one into the other at specific sites. The parameters used for the modelling were based on estimates from experimental quantitative measurements of mRNA translation in eukaryotic systems.

The application of the model has demonstrated that indeed a small subset of specific uORFs (constrained by length and leakiness of their initiation sites) are capable of upregulating translation downstream in response to the reduced TC availability, which is observed under ISR. Here we describe the computer simulations based on this model and discuss the implications of our results to understanding naturally occurring uORF-mediated stress resistance.

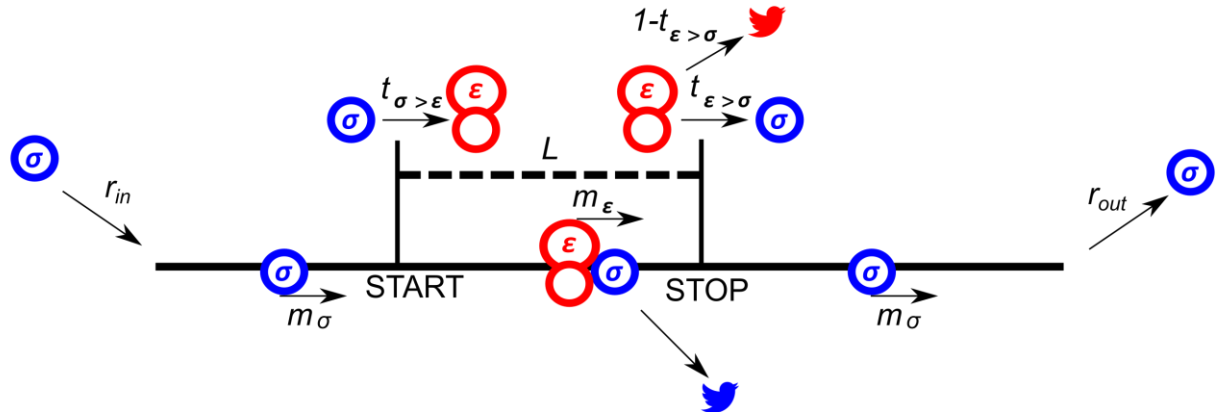
RESULTS

The model of Initiation Complexes Interference with Elongating Ribosomes (ICIER)

The ICIER model and its parameters are illustrated in Figure 1. Each site of the TASEP lattice represents a codon. All sites have the same properties except two that represent the start and the stop codons of the uORF. There are two types of particles, scanning ribosomes (σ) and elongating ribosomes (ϵ). Each particle occupies 10 codons in accordance with the predominant mRNA length protected by elongating ribosomes (25,46,47). For simplicity, in our default model scanning ribosome size is the same even though scanning complexes have been shown to protect mRNA fragments of different lengths (48). These ribosomes can move forward by a single unoccupied site with probabilities m_σ and m_ϵ . In addition, scanning ribosomes can transform into elongating ribosomes at the start site with a probability $t_{\sigma \rightarrow \epsilon}$, which may vary from 0 (no initiation) to 1 (non-leaky initiation). At the stop site, elongating ribosomes could transform into scanning ribosomes with a probability $t_{\epsilon \rightarrow \sigma}$ allowing for reinitiation. The remaining elongating ribosomes terminate (disappear) with the probability $1 - t_{\epsilon \rightarrow \sigma}$. We hypothesized that scanning ribosomes would dissociate from mRNA when upstream elongating ribosomes collide with them. This hypothesis is based on the following considerations. When moving scanning ribosomes collide with other ribosome complexes, they may stay on the mRNA or dissociate. In the latter case we can consider four possibilities. A scanning ribosome dissociates when it encounters a ribosome complex downstream, scanning (option #1) or elongating (option #2). Alternatively, an upstream complex (either scanning #3 or elongating #4) could cause dissociation of a scanning ribosome. The options that scanning ribosome collision cause dissociations (#1 and #3) would make formation of scanning ribosome queues impossible. However they have been observed upstream of start sites in yeast (48). Also it has been demonstrated recently that an elongating ribosome pause downstream of a weak initiation site stimulates translation initiation (49). This seems possible only if scanning (and/or elongating) ribosomes could queue upstream of elongating ribosomes. This evidence makes option #2 also unlikely. Therefore, the only remaining option is that scanning ribosomes do not frequently dissociate from mRNA but they do when the collision occurs with the elongating ribosome upstream (#4). Therefore, we used these conditions as default in our simulations. Nonetheless, we also explored how alternative scenarios (no

dissociation and spontaneous dissociation of scanning ribosomes) affect the ability of uORFs to provide the stress resistance in this model (see subsection “Miscellaneous parameters of the model: ribosome gabarits and fall off rates”).

A



B

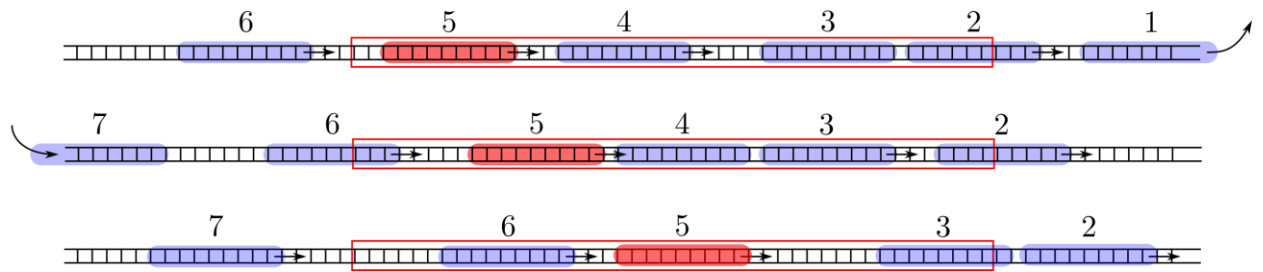


Figure 1. ICIER model. **A.** Parameters of the model. The lattice is shown as a black line with the positions of start and stop codons separated by L sites (codons). Scanning ribosomes are blue and elongating are red in both panels. Ribosome dissociation from mRNAs are indicated with bird symbols. **B.** An example of three subsequent states of the lattice with ribosomes shown as semitransparent oval shapes and each ribosome is labeled with a unique index. Arrows indicate changes between current and subsequent steps. The red rectangle specifies the location of the uORF.

Using ICIER under different parameters we explored how the rate of scanning ribosomes arriving at the end of the lattice r_{out} depends on the rate with which scanning ribosomes are loaded at the beginning of the lattice r_{in} . r_{in} corresponds to the rate of PIC assembly at the 5' end of mRNA that depends on TC availability which is reduced upon eIF2 phosphorylation. r_{out} corresponds to the rate of scanning ribosomes arrival to the start of the acORF. In essence, upregulation of acORF translation under stress in terms of our model means an increase in r_{out} in response to a decrease in r_{in} .

The effect of uORF length on the flux of scanning ribosomes

First, we explored how the rate of PIC loading (r_{in}) affects the density of scanning ribosomes downstream (r_{out}) of a uORF depending on its length (L). The results of a typical simulation for a set of specific parameters are shown in Figure 2. For these simulations the possibility of reinitiation was excluded ($t_{\sigma>\epsilon} = 0$). To allow for leaky scanning the strength of uORF translation initiation was set $t_{\sigma>\epsilon} = 0.8$ (80% of scanning ribosomes convert to elongating ribosomes at the start of the uORF). The rate of elongation in all simulations was modelled as 0.3 probability that the ribosome moves during a single tact ($m_{\sigma} = 0.3$). Assuming that an average mammalian ribosome moves 5 codons per second during elongation (20), the tact of simulation would correspond to 0.06 seconds (0.3/5). We were unable to find experimental estimates for the velocity of scanning ribosomes *in vivo*, but *in vitro* estimates are similar to that of elongating ribosomes (50,51). Hence, for the simulations shown in Figure 2 we used

equal rates for elongating and scanning ribosomes ($m_e = 0.3$). To simulate stress conditions, we tested the model under variable r_{in} from high to absolute zero. It has been estimated that in yeast, on average, the ribosome loads onto mRNA every 0.8 seconds (52), which in terms of our model would be a probability of ribosome load 0.075 per tact. Thus, we decided to model the behavior of the system in the range from 0.1 to 0 (Figure 2). In the absence of uORFs, the r_{out} correlates with r_{in} although non-linearly (Fig.2A,B yellow). At the onset of stress, the decrease in r_{in} leads to a disproportionately small decrease in r_{out} , but at a near zero value of r_{in} , the rates r_{in} and r_{out} begin to decrease proportionally. This is because of changes in the likelihood of ribosome collisions that reduce their flow. When the load rate is close to zero, very few ribosomes traverse mRNA making collisions highly unlikely and leading to a direct relationship between r_{in} and r_{out} . It appears that the addition of even very short ORFs substantially reduces the number of ribosomes downstream (Fig. 2B). This is not surprising, in the absence of reinitiation at least 80% of scanning ribosomes would be lost. Most interestingly, once the uORF reaches a certain length (between 20 and 30 codons in simulations shown in Fig. 2) the relationship between r_{in} and r_{out} becomes non-monotonous and r_{out} starts to increase with decreasing r_{in} at a certain interval. The effect is much more profound for longer uORFs (Fig. 2A,C). However, this advantage afforded by a uORF in stress resistance comes at a price - as can be seen from Figure 2B, uORF containing mRNAs have lower levels of r_{out} when r_{in} is high and this repression increases with uORF length (Fig. 2D). This occurs due to increasing incidence of collisions by scanning and elongating ribosomes within the uORF and subsequent dissociation of scanning ribosomes.

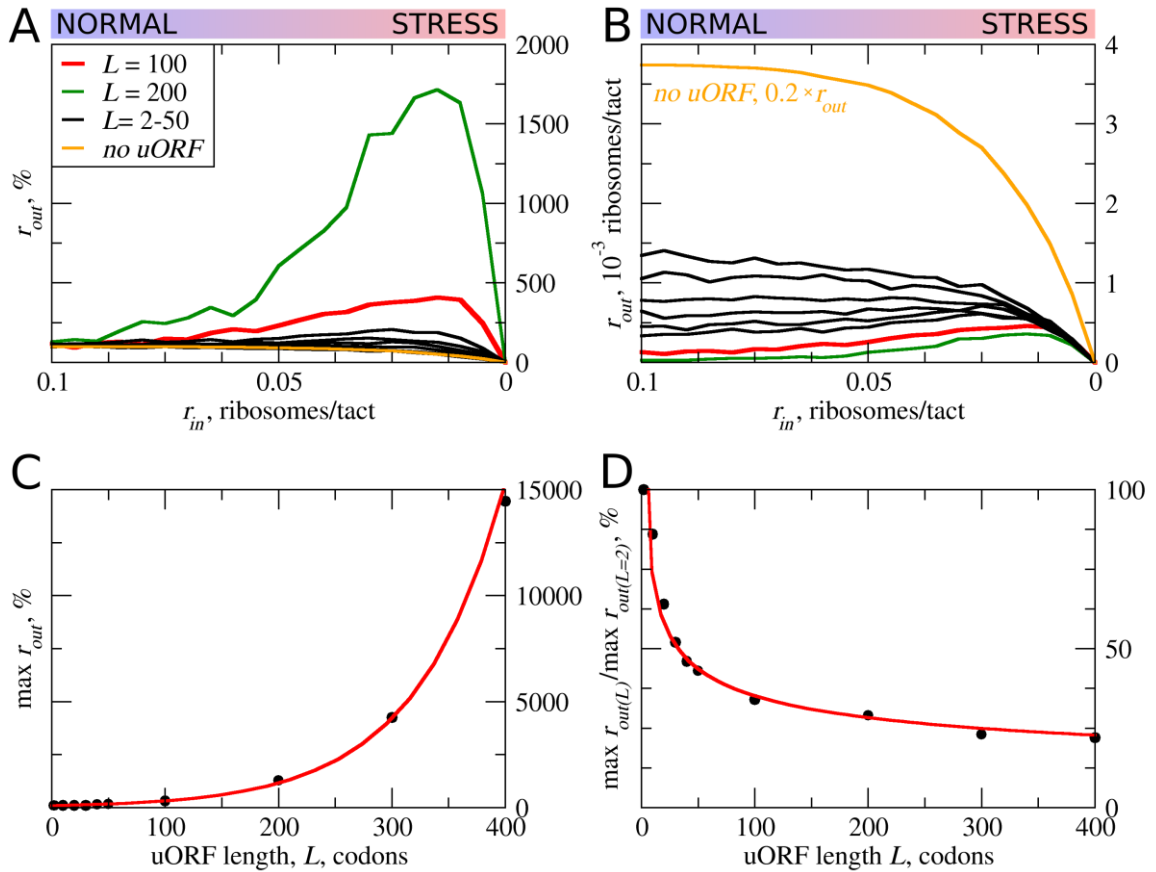


Figure 2. uORF length (L) influences how the flux of scanning ribosomes changes downstream (r_{out}) in response to lowered ribosome load (r_{in}) due to stress. Other parameters of the simulations $t_{e>\sigma} = 0$; $t_{\sigma>e} = 0.8$; $m_{\sigma} = m_e = 0.3$. **A, B.** Relative ($r_{out}(r_{in})/r_{out}(r_{in}=0.1)$) (A) and absolute (B) changes in the density of ribosomes downstream of a uORF for a range of r_{in} from 0.1 to 0 for mRNAs containing uORFs of different lengths (L). **C.** Dependence of the relative (r_{out}) maximum on the uORF length. **D.** The decrease of maximum r_{out} as a result of increasing uORF length

(maximum r_{out} for each L is normalized by r_{out} for $L=2$). Source data for panel A are provided in Figure 2–Source Data 1 and for panel B in Figure 2 – Source Data 2.

In other words, according to our ICIER model, long uORFs repress translation of downstream ORFs which are de-repressed during stress. This is consistent with our earlier study, where we found that the best predictor of stress resistant mRNAs is the presence of an efficiently translated uORF combined with very low translation of the downstream acORF (26).

The effect of uORF elongation rate on the flux of scanning ribosomes

In the simulations described above the movement rates of scanning and elongating ribosomes were set to be equal. However, codon decoding rates can vary significantly depending on their identity and surrounding sequences (for example, see (53-55)). Thus, the average elongation rate could also vary for different uORFs. This is particularly salient where uORFs encode stalling sites such as in *DDIT3* (39). Therefore, we explored how variations in the rate of ribosome elongation affect the behavior of our model. Even a small decrease in the elongation rate (m_e) strongly increases the maximum r_{out} relative to its basal level (Fig. 3). The global (sequence non-specific) rate of elongation may be decreased by stress (for example, by eEF2 phosphorylation) contributing to the stress resistance granted by uORFs. Perhaps, more importantly, the local decoding rates may be specifically tuned to the uORF sequences, through nascent peptide mediated effects or *via* RNA secondary structures in 5' leaders.

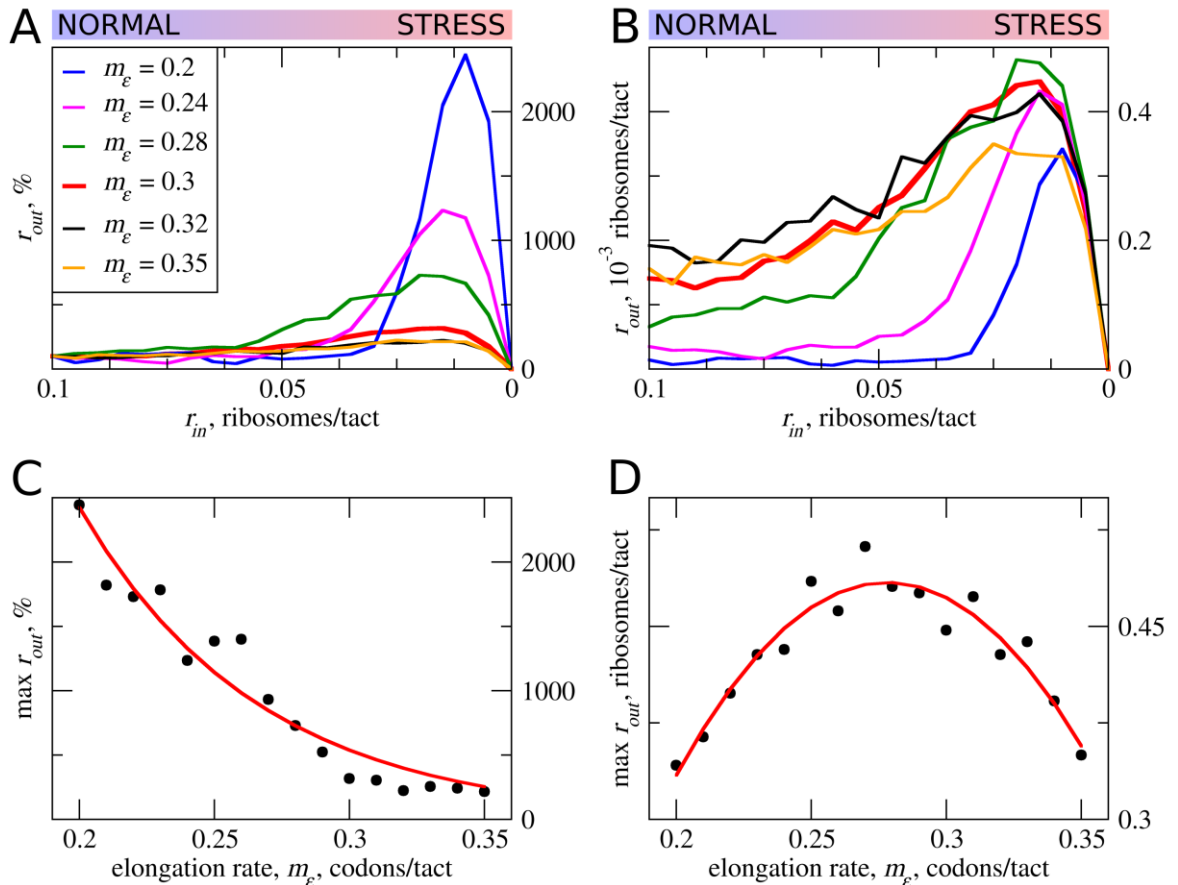


Figure 3: The effect of elongating ribosomes movement rates (m_e) on stress resistance. Other parameters of the simulations $t_{\epsilon > \sigma} = 0$; $t_{\sigma > \epsilon} = 0.8$; $L = 100$; $m_{\sigma} = 0.3$. **A, B.** Relative ($r_{out}(r_{in})/r_{out}(r_{in}=0.1)$) (A) and absolute (B) changes in the density of ribosomes downstream of the uORF for a range of r_{in} from 0.1 to 0 for different elongating ribosome movement rates (m_e are indicated). **C.** Dependence of the relative (r_{out}) maximum increase on elongating ribosome

movement m_e . D. Dependence of the absolute maximum r_{out} rate on the m_e . Source data for panel A are provided in Figure 3–Source Data 1 and for panel B in Figure 3 – Source Data 2.

Whereas the stress resistance monotonously increases with decreased elongation rates (Fig. 3C), the absolute r_{out} maximum is not monotonous and reaches a maximum when elongating ribosomes are slightly slower than scanning ones (Fig. 3D). This clearly points to a tradeoff similar to that observed for uORF lengths: the more slowly decoded uORFs provide higher resistance to the stress, but at a cost of higher uORF-mediated repression under normal conditions, thus requiring more mRNA molecules for the same protein synthesis rate. However, if scanning ribosome speed greatly exceeds that of elongating ribosomes, the increased inhibition under normal conditions does not convert into stress resistance. Relative r_{out} , as well as absolute r_{out} rates drop with increased elongating ribosome velocities once they approach the velocity of scanning ribosomes (Fig. 3A,B).

It is not clear whether the rates of scanning ribosomes can be influenced locally by nucleotide sequences or whether it can vary under the stress conditions. According to the ICIER modelling, for a maximal performance of uORF containing mRNAs under stress there should be optimal ratio of scanning to elongating ribosomes velocities. Thus, we can hypothesize that not only codon composition of uORF affecting local decoding rates, but also its primary sequence, which may affect local scanning rates, may be important determinant of uORF function.

Strength and pausing of translation initiation at uORFs and the probability of reinitiation downstream

Translation initiation could often be leaky depending on the context. In this case only a proportion of ribosomes initiate at a start codon, while the remaining ribosomes continue scanning (2,56). This is particularly relevant to uORFs, since even a very weak start codon would yield detectable translation when there are no start codons upstream of it that would reduce the pool of scanning ribosomes (18). Thus, many known regulatory uORFs are initiated at non-AUG starts (15,22,27,49). As expected, increased leakiness of the uORF start (lower $t_{e>o}$) elevates the flow of ribosomes downstream of the uORF (Figure 4A). The stress resistance is also reduced considerably for uORFs with leaky starts and disappears when only 30% or less initiate at the uORF in the context of other parameters used for the simulations shown in Figure 4A-D. This allows us to speculate that uORFs with non-AUG start codons unlikely would be able to provide stress resistance, as such initiation codons are non-optimal by default and should be prone to leaky scanning.

Our default model does not take into account that initiation is a slow process. It is conceivable that the time that the initiating ribosome spends on the start codon may affect the stress resistance and it is likely that this initiation dwell time may vary for different start codons. We therefore carried out simulations in which elongating ribosomes were paused at the start immediately after their conversion from scanning ribosomes. The length of delay was set as a probability $\delta\epsilon$ that determines the ability of paused elongating ribosomes to move (Fig. 4E,F). Apparently, the increased delay reduces the inhibitory effect of uORFs and reduces the stress resistance. This is an expected result in the context of the model, since the delay of initiating ribosomes increases its distance to the downstream scanning ribosomes and thus reduces the chance of the collision.

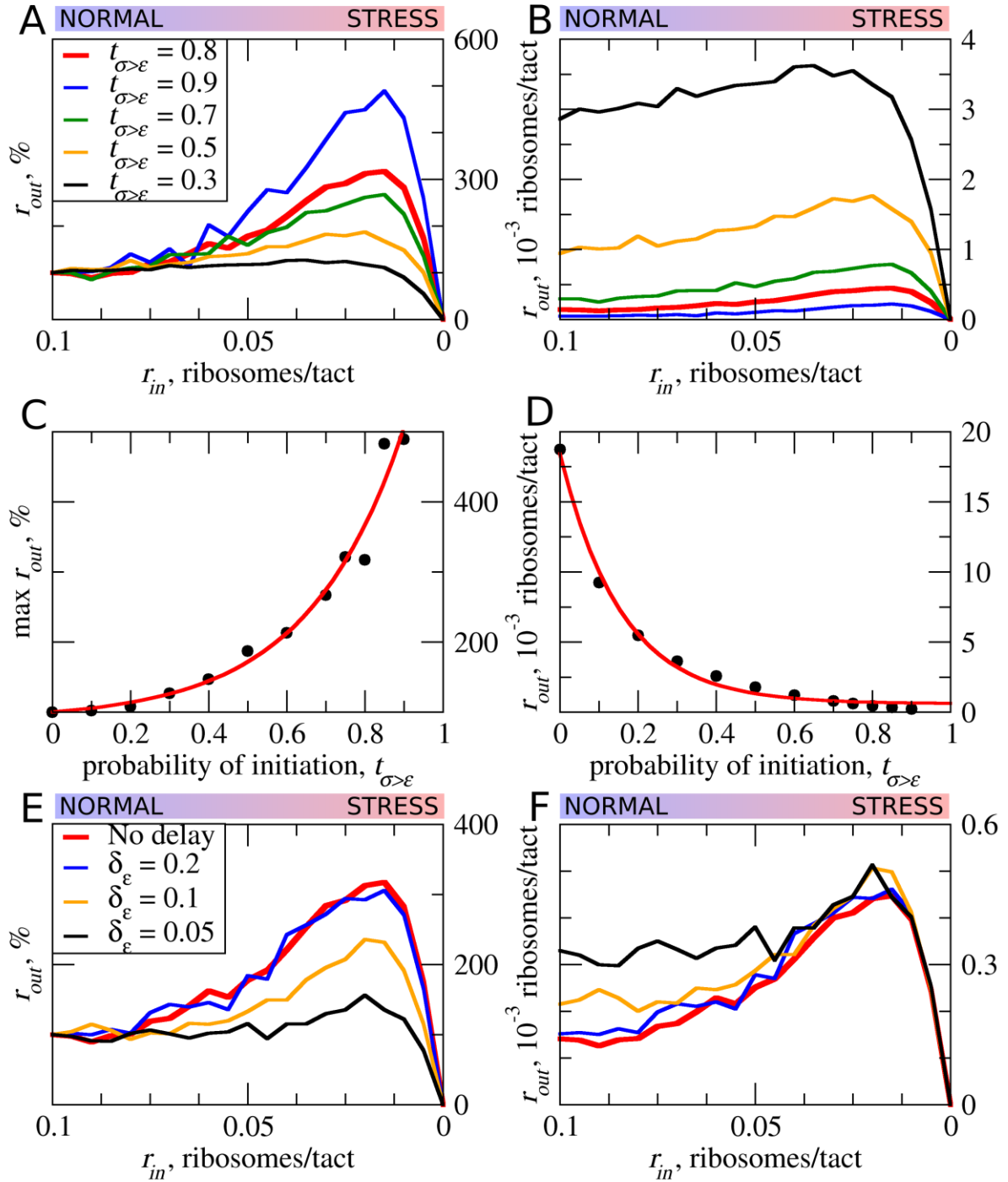


Figure 4: The effect of uORF initiation efficiency ($t_{\sigma>\epsilon}$) on stress resistance. Other parameters of the simulations $t_{\epsilon>\sigma} = 0$; $L = 100$; $m_{\sigma} = 0.3$; $m_{\epsilon} = 0.3$. **A, B.** Relative ($r_{out}(r_{in})/r_{out}(r_{in}=0.1)$) (A) and absolute (B) changes in the density of ribosomes downstream of a uORF for a range of r_{in} from 0.1 to 0 for different uORF initiation efficiencies ($t_{\sigma>\epsilon}$ are indicated). **C.** Dependence of the relative (r_{out}) maximum increase on the uORF initiation efficiency $t_{\sigma>\epsilon}$. **D.** Dependence of absolute maximum r_{out} rate on the $t_{\sigma>\epsilon}$. **E, F.** Relative ($r_{out}(r_{in})/r_{out}(r_{in}=0.1)$) (E) and absolute (F) changes in the density of ribosomes downstream of a uORF depending on the delay $\delta\epsilon$ which is the probability that newly formed elongating will move. For no delay $\delta\epsilon = 1$. Source data for panel A are provided in Figure 4 – Source Data 1, for panel B in Figure 4 – Source Data 2, for panel E in Figure 4 – Source Data 3 and for panel F in Figure 4 – Source Data 4.

In all of the above simulations reinitiation of ribosomes terminating at the uORF was disallowed, i.e. $t_{\epsilon > \sigma} = 0$. In practice, however, a significant proportion of ribosomes can reinitiate downstream depending on specific uORF features (32,57,58). Intuitively, uORFs that allow reinitiation downstream should be less inhibitory, e.g. when all ribosomes reinitiate downstream of the uORF with an optimal non-leaky start all ribosomes engaged with mRNA would also translate aORF. It is therefore also likely that reinitiation would reduce the ability of uORF to provide stress resistance. We explored how reinitiation affects stress resistance in the context of the ICIE model (Figure 5) by permitting terminating ribosomes to convert to scanning ribosomes with a certain probability. As expected, elevated reinitiation reduces the inhibitory effect of uORFs as well as the stress protective effect of uORFs. It appears that a dramatic effect could be achieved even at very low reinitiation rates. In the simulations shown in Figure 5 the significant reduction of stress resistance can be observed with a reinitiation rate as low as 1% and the resistance almost disappears when just 5% of the ribosomes reinitiate downstream. Based on these observations we predict that single uORFs that enable stress resistance do not allow reinitiation to take place unlike in the case of mRNAs with a combination of uORFs achieving a protective effect through delayed reinitiation as in GCN4 (31).

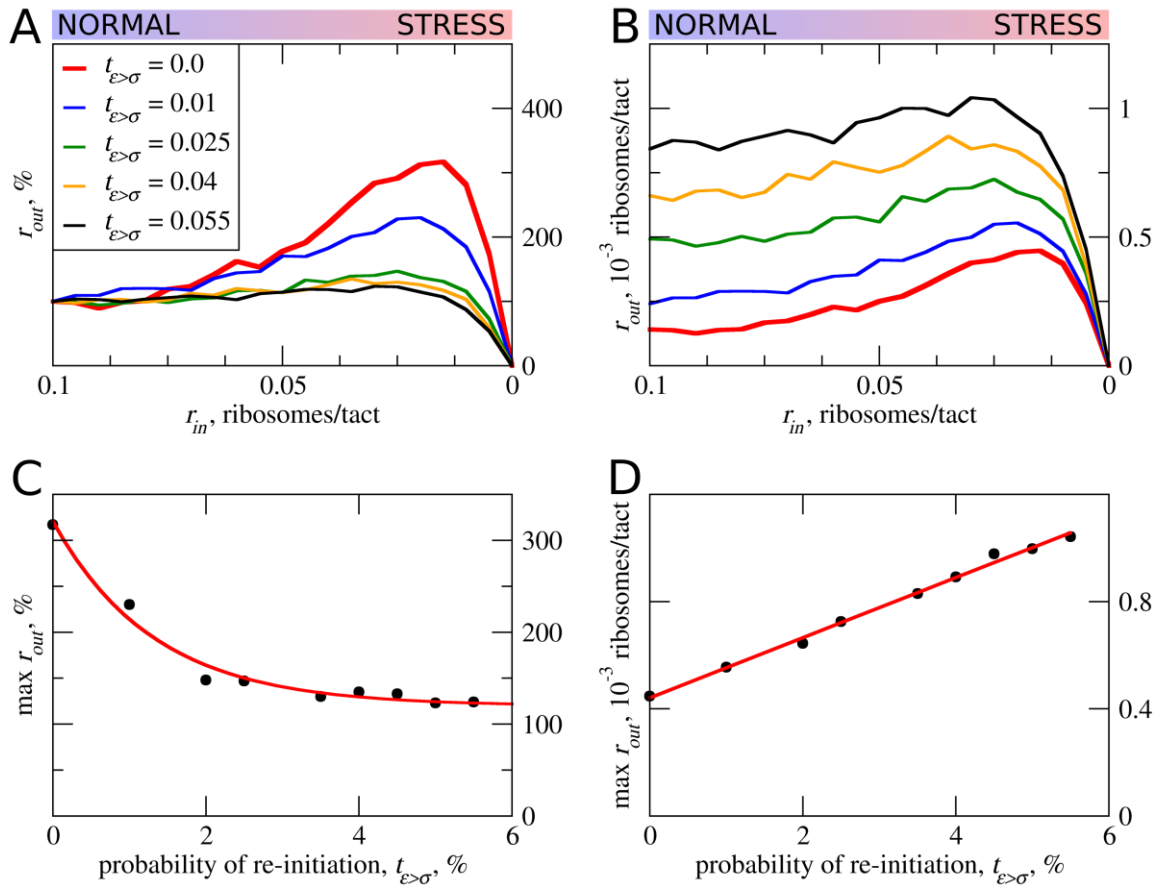


Figure 5: The effect of reinitiation downstream of the uORF on stress resistance. Other parameters of the simulations $t_{\epsilon > \sigma} = 0$ $t_{\sigma > \epsilon} = 0.8$; $L = 100$; $m_{\sigma} = 0.3$; $m_{\epsilon} = 0.3$. **A, B.** Relative ($r_{out}(r_{in})/r_{out}(r_{in}=0.1)$) (A) and absolute (B) changes in the density of ribosomes downstream of a uORF for a range of reinitiation probabilities ($t_{\epsilon > \sigma}$ from 0 to 0.055 as indicated). **C.** Dependence of the relative (r_{out}) maximum increase on the reinitiation probability $t_{\epsilon > \sigma}$. **D.** Dependence of absolute maximum r_{out} rate on the $t_{\epsilon > \sigma}$. Source data for panel A are provided in Figure 5–Source Data 1 and for panel B in Figure 5–Source Data 2.

Miscellaneous parameters of the model: ribosome gabarits and fall off rates

So far, in all simulations the only condition when scanning ribosomes dissociated from mRNA was when colliding with upstream elongating ribosomes. However, the complexes of scanning ribosomes with mRNA are unstable as their co-isolation with mRNA requires chemical cross-linking (48,59). It is therefore likely that scanning ribosomes dissociate from mRNA even in the absence of collisions with other ribosomes. It is unclear what are the factors affecting the stability of scanning ribosomes in complex with mRNA, for example, it does not seem that the length of 5' leaders have a substantial effect on the probability of scanning ribosomes to dissociate from mRNA (50,60). Without adequate knowledge of the factors influencing the dissociation of scanning ribosomes from mRNA we decided to model it as spontaneous dissociation from mRNA using varying dissociation probabilities. First, we explored how such spontaneous dissociation affects our default model when scanning ribosomes are being removed by upstream elongating ribosomes (Fig. 6A). It appears that such spontaneous dissociation do not significantly affect the inhibitory effect of uORFs, but they reduces their stress protective properties.

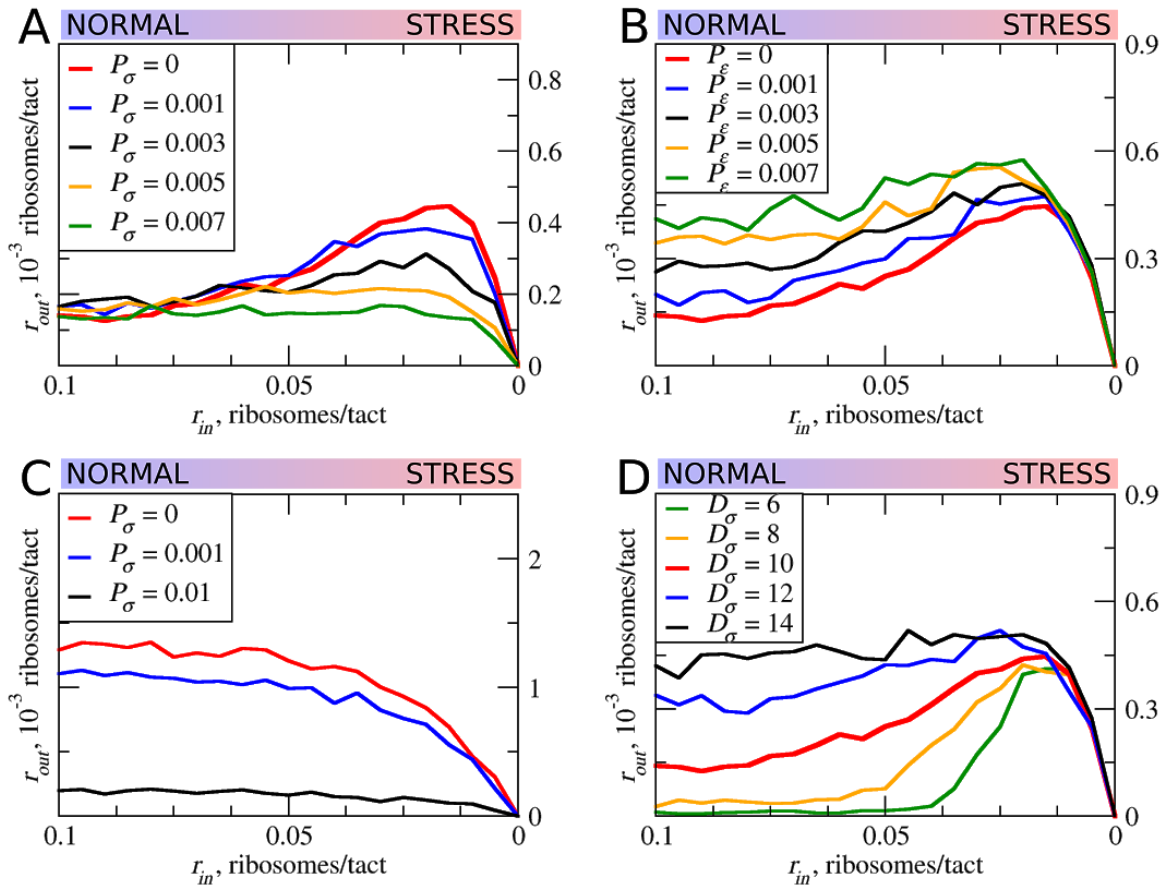


Figure 6: The effect of the size of scanning ribosomes D_σ and probability of spontaneous ribosome dissociation P_σ on stress resistance. Other parameters of the simulations; $t_{\sigma\epsilon} = 0.8$; $L = 100$; $m_\sigma = 0.3$; $m_\epsilon = 0.3$. **A, B.** Absolute changes in the density of ribosomes downstream of a uORF under a scenario where scanning (A) or elongating (B) ribosomes could dissociate spontaneously with probabilities P_σ and P_ϵ respectively. **C.** Same as B but scanning ribosomes do not dissociate upon collisions with elongating ribosomes. **D.** The absolute changes in the densities of ribosomes downstream of a uORF depending on the size of scanning ribosomes. Source data for panel A are provided in Figure 6–Source Data 1, for panel B in Figure 6 – Source Data 2, for panel C in Figure 6 – Source Data 3 and for panel D in Figure 6 – Source Data 4.

Although elongating ribosome drop off is very low in mammals (61) and even in bacteria (62,63), we explored how different rates of drop-off could affect behavior of our model. It appears that increased drop-off reduces both, inhibitory and stress protective properties of uORFs (Fig. 6B).

Further we explored how the system would behave if scanning ribosomes would dissociate only spontaneously, i. e. collisions do not cause dissociations (Fig. 6C). In this case, uORFs lose any stress protective properties.

Ribosome structures are dynamic and they undergo conformational changes as they move along mRNA, for example, they protect mRNA fragments of different size depending on whether the POST- or PRE-translocation complex is being stabilized (64). Scanning ribosomes also change the length of protected fragments depending on their conformations and the influence of translation initiation factors associated with it (48,65). To explore how the length of the space that ribosomes occupy on mRNA influences our model, we carried out a series of simulations where the length of elongating ribosomes was kept constant at 10 codons, while the length of scanning ribosomes was varied (Fig. 6D). Counterintuitively, we observed substantial differences. The inhibitory effect of uORFs and their stress protective properties appears to be much higher in the case of “short” scanning ribosomes. Without knowledge of mechanistic aspects of ribosome collisions and its consequences this observation gives us little except for the fact that the dimensions of scanning and elongation ribosomes are important parameters which can influence the uORF performance under stress.

Correlations with existing ribosome profiling data.

While our model cannot make accurate predictions of stress resistance levels for specific mRNAs, it makes certain predictions regarding the general features of uORFs associated with stress protective properties of uORFs occurring in mRNA 5' leaders not containing other uORFs. Specifically, according to our model, stress protective uORFs should not permit significant reinitiation downstream. Longer uORFs are expected to be more protective than short uORFs and those that are initiated more efficiently should be more stress protective than those poorly translated. In addition, uORFs containing slowly decoded regions should also be stress-protective. To explore whether these predictions hold true we focused on the data obtained in three independent studies carried out in HEK293T cells where the ISR was inflicted either with arsenite (26,66) or tunicamycin treatments (30).

For these purposes we selected 325 transcripts containing single uORFs whose translation is supported by aggregated ribosome profiling data from the same studies that are currently publicly available in the GWIPS-viz browser (67,68). We then correlated the features of these uORFs with the stress resistance of their corresponding mRNAs that was estimated as a Z-score upon Z-score transformation as in our earlier studies (22,26), see Methods. The measurement of uORF length is straightforward, it was calculated as the number of codons between the first ATG codon of a uORF and its stop codon. Indeed, as predicted by the model we found strong and statistically significant positive correlation between uORFs and stress resistance of their corresponding mRNAs in all three studies (Fig. 7A). To estimate the efficiency of translation of uORFs we measured their ribosome occupancy under control conditions, see Methods. This was made under the assumption that the translation initiation efficiency of a uORF is a major factor determining the average density of footprints aligning to that uORF. We found positive and statistically significant correlations between uORFs' footprint densities and their stress protective properties only in one of the three studies (Fig. 7B). To estimate the presence of ribosome pauses in uORFs we compared the magnitude of the highest peak of density in the uORF relative to its average footprint density using transcriptome alignments of the data from the studies available in GWIPS-viz (68), see Methods. While we observed positive correlations between pause scores and stress resistance in all three studies, they appeared weak and not statistically significant (Fig.

7C). There are several possible explanations for the lack of statistically significant correlations between average footprint densities, pause scores and stress resistance which do not necessarily invalidate the predictions of our model. First, it is expected that our estimates of initiation and pausing based on ribosome profiling data are not sufficiently accurate due to short lengths of uORFs, mappability and sequencing biases (69). Second, the selection of mRNA with single uORFs necessitated the choice of uORFs that fits only a certain range of property parameters, e.g. if a uORF's translation efficiency is low we may not be able to detect such a uORF as being translated. Finally, the distribution of uORFs with different features is intrinsically non-random due to evolutionary selection imposed by functional properties of uORFs. Nevertheless, the observation that uORF length is important and is a significant determinant of stress resistance supports the results of ICIER modelling. In all 3 studies, uORF containing mRNAs with high Z-score (>2) are completely depleted for very short uORFs which, under our simulations, are not able to provide stress resistance due to ribosome collisions.

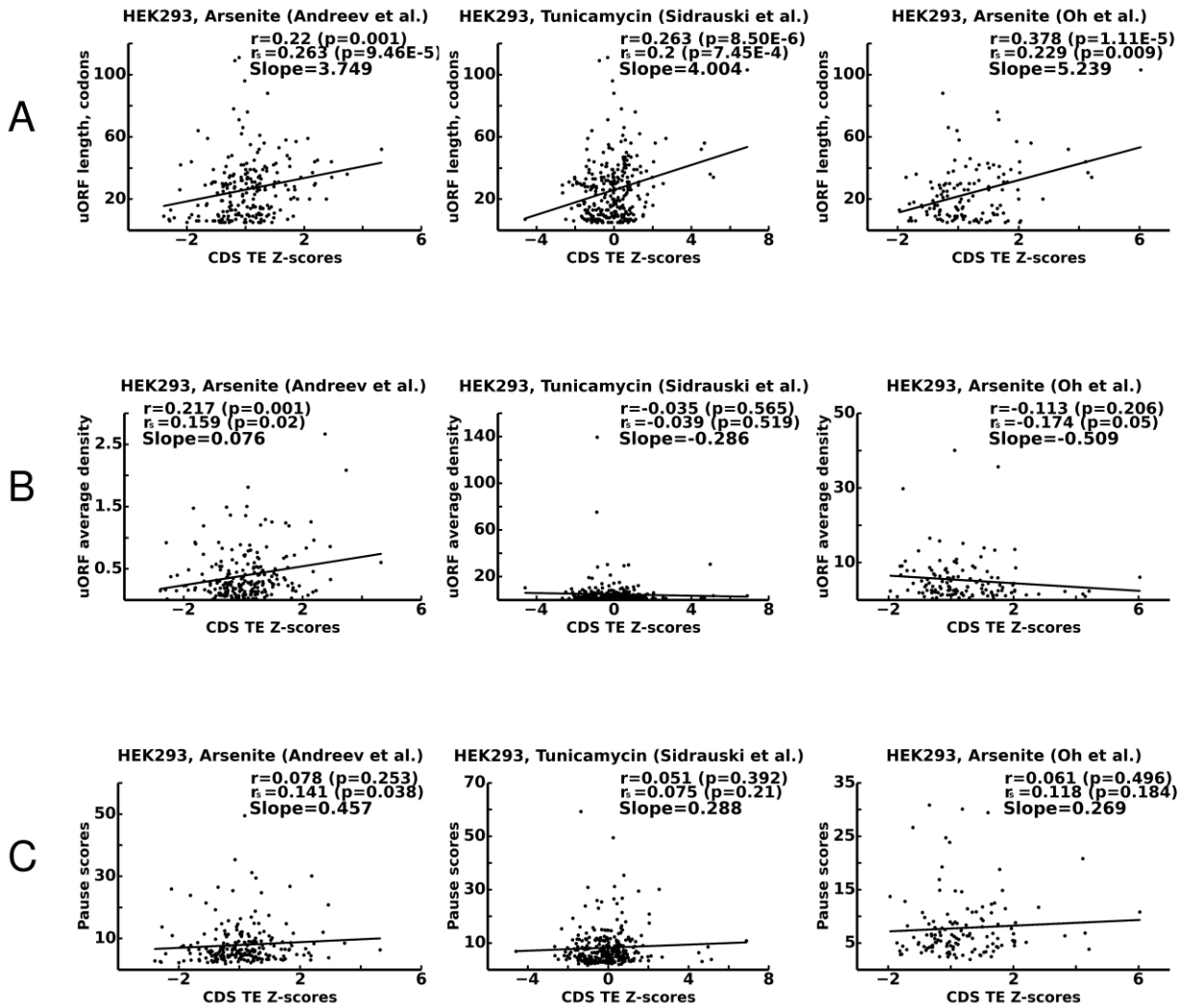


Figure 7: Correlations between translational stress resistance of mRNAs (axis x) and features of uORFs in their 5' leaders (axis y) for three studies (indicated above each plot). A. uORF length. B. uORF translation initiation measured as uORF translation efficiency. C. Ribosome pausing estimated with pause score. Pearson correlation coefficients (r) and Spearman rank correlations (r_s) are provided in the figure for each plot along with corresponding p-values. The slope of linear regression is also indicated for each plot. Source data are provided in Figure 7–Source Data 1.

DISCUSSION

Using the ICIER model developed in this work we explored how the flow of scanning ribosomes across mRNA leader is changed in the presence of a translated ORF depending on several parameters such as ORF length, initiation efficiency, decoding rate and reinitiation probability. Our results demonstrate that for mRNAs with certain uORFs the relationship is not monotonous. It appears that within a certain range, the rate of PIC assembly has an inverse relationship with ribosome availability downstream of uORFs. We explored how several different parameters of uORFs affect this phenomenon. It appears that the non-monotonous behavior emerges only after uORFs reach a certain length. The elevation of ribosome flow downstream of a uORF is higher for longer uORFs. However, uORF inhibitory effects on downstream translation also increase with their length. Thus, there is a clear trade-off: while longer uORFs provide stronger resistance to the stress, the translation efficiency under normal conditions is lower for ORFs downstream of longer uORFs. Consequently, to achieve the same protein synthesis rate more mRNA copies need to be synthesized. This trade-off likely shapes the specific lengths of regulatory uORFs and the steady state levels of corresponding mRNAs.

Decreased elongation rates increase the stress resistance. A global decrease in elongation rates is expected under certain stress conditions, for example, due to eEF2K-mediated phosphorylation of eEF2 (70) or due to decreased concentration of available aminoacylated tRNAs. However, the decoding rates may vary among different uORFs since specific sequences affect the speed of the elongation. Indeed, it seems that at least some stress resistant mRNAs contain stalling sites (39). It should be noted that slow elongation at the uORF is also at cost, there is a tradeoff between absolute levels of translation under stress and slow elongation. Interestingly, the optimal performance of uORF as a stress resistor seems to be achieved under certain ratio between scanning and elongation ribosome velocities.

In all of the above simulations, irrespective of the specific parameters used, the stress resistance (when observed) occurred within a specific narrow range of scanning ribosome loading on mRNA ($r_{in} \sim 0.02$). It is reasonable to expect that stress resistance of specific mRNAs would be tuned to particular levels. We equated stress levels to r_{in} rates, but it is likely that different mRNAs have different r_{in} rates under the same cellular conditions. The exact sequence at the 5' end of mRNA may potentially influence eIF4F assembly (71) and subsequently the rate with which the PIC is assembled on mRNA. Indeed, the effect of mRNA 5' end on single uORF dependent stress resistance was recently demonstrated (26): an addition of a strong hairpin to the 5' end of *IFRD1* leader alleviated stress resistance even though the uORF itself was remained intact. Also, according to our simulations, leaky initiation at uORF starts reduces stress resistance, as well as the possibility of re-initiation downstream of the uORF. This highlights the importance of uORF flanking sequences (upstream - for modulating PIC recruitment (Rin) and initiation efficiency, and downstream – for reinitiation) on uORF performance. Thus, despite the central role of uORF, other sequences of 5' leader can significantly influence mRNA translation under stress as well.

To validate our model, we explored how uORF features correlate with stress resistance of mRNAs using ribosome profiling data obtained under stress conditions in studies from three independent laboratories (26,30,66). We found that uORF length strongly correlates with its stress protective properties. While the model predicts that the efficiency of translation initiation should also correlate with stress protective properties of uORFs, we found support for this prediction in only one of the three studies (26). Only weak and statistically insignificant correlations were found between the strength of ribosome pauses in uORFs and stress resistance. Besides technical difficulties in estimating translation initiation efficiency and elongation rates from ribosome profiling data, the relationship of the last two parameters and stress resistance may be convoluted by non-random features of naturally occurring uORFs. More “uORF centered” experimental approach is required to explore the details uORF functions under stress, e.g. with ribosome profiling under conditions of various degree of ISR (PIC depletion), with precise mapping of 5' leaders (which can be achieved with nano CAGE) to uncover more

mRNA species with single uORF, and with very deep coverage for more accurate uORF riboseq signal quantification.

In conclusion, by using a simple model of scanning and elongating ribosome interference we demonstrated that a single uORF can be sufficient for providing mRNA translation control with resistance to TC depletion which occurs during ISR. The general principle of uORF mediated stress resistance seems to be based on strong repression of downstream translation under normal conditions which is derepressed during the stress. The exact parameters of stress protective uORFs are thus a product of the trade-off between the inhibition of absolute levels of translation and its relative increase during the stress. The uORFs providing the resistance are likely to be longer, their initiation sites are expected to have low level of leakiness (but some level of leakiness is essential), they may contain slowly decoded sites and they should not permit high levels of reinitiation downstream. Given that a single uORF could be such a versatile regulatory element, a combination of regulatory uORFs could generate very complex behaviors. Many eukaryotic mRNAs contain multiple uORFs and their concerted impact should be the subject of future experimental and theoretical studies. Obtaining accurate values for ICIER modelling and further improvements of the model may eventually aid the design of mRNA leaders with the desired response to stress.

METHODS

ICIER implementation and computer simulations

The mRNA was modeled by a string of $L=L_1+L_2+L_3$ symbols 0, 1, 2 with uORF modeled by the L_2 symbols in the middle part of the string. Symbol 0 corresponds to an unoccupied site (codon). A block of D_σ consecutive symbols 1 corresponds to D_σ sites occupied by a scanning ribosome. A block of D_ϵ consecutive symbols 2 corresponds to D_ϵ sites occupied by an elongating ribosome.

At every tact (time step), the code implements several routines modeling the random processes described in the subsection “The model of Initiation Complexes Interference with Elongating Ribosomes (ICIER)”: attachment of scanning ribosomes to the mRNA, ribosomes movement, dissociation of ribosomes from the mRNA, initiation of scanning ribosomes and reinitiation of elongating ribosomes. More precisely, one time-step of the algorithm includes the following routines:

1. If there are at least D_σ unoccupied sites at the beginning of the mRNA, then the algorithm adds a scanning ribosome to the first D_σ sites with probability λ (by changing the first D_σ symbols 0 to 1).

2. If the end symbol 1 of a scanning ribosome is at the initial site of uORF and (in case $D_\epsilon > D_\sigma$) there are enough unoccupied sites to fit an elongating ribosome, then this scanning ribosome is replaced with an elongating ribosome with probability $P_{\sigma \rightarrow \epsilon}$.

3. If the end symbol 2 of an elongating ribosome is at the last site of uORF and (in case $D_\epsilon < D_\sigma$) there are enough unoccupied sites to obtain a scanning ribosome, then the elongating ribosome is replaced with a scanning ribosome with probability $P_{\epsilon \rightarrow \sigma}$ and is dissolved with probability $1 - P_{\epsilon \rightarrow \sigma}$.

4. A scanning ribosome reaching the last site of mRNA is removed from the mRNA (by changing 1s to 0s), and the algorithm registers this ribosome as reaching the final position.

5. At every other site of the mRNA every ribosome either moves or stays according to the following rules:

- a. A scanning ribosome moves one step forward with probability P_s if there is an empty site in front of it.

b. An elongating ribosome moves one step forward with probability P_s if the site in front of it is not occupied by an elongating ribosome. If the site in front of a moving elongating ribosome is 1 meaning that there is a scanning ribosome in front of it, then this scanning ribosome is removed from the mRNA.

6. Each scanning and elongating ribosome is removed from the mRNA with probability Q_s and Q_e , respectively.

The algorithm was implemented in the MATLAB software package. The simulations were performed on a standard MacBook computer.

Each data point for Figures 1—6 was generated by running the code for 10^6 time steps. A typical curve in these figures contains 20 data points corresponding to different values of the loading probability λ (r_{in}).

The computer code is freely available at GitHub:
https://github.com/maximarnold/uORF_TASEP_ICIER (72)

Parameters of all simulations described in this manuscript and their outcomes are provided in Supplementary File 1.

Analysis of ribosome profiling data.

For the detection of reliably translated upstream open reading frames (uORFs) data aggregated from a subset of the studies currently available in GWIPS-viz browser(68) were used. Specifically, the data were pulled from the following studies (26,30,61,66,73-79). APPRIS principal isoforms (80) with annotations from Gencode version 25 were used. All ORFs located within the 5' leader of Gencode transcripts not overlapping CDS were ranked based on their translational efficiency. The top 5% were manually examined for the consistency of ribo-seq signal and the absence of other translated regions in the 5' leaders. mRNAs with more than one uORF were excluded from the analysis. In total 325 transcripts were accepted as transcripts with a single uORF. Gencode transcript IDs and the coordinates of uORFs are provided in Supplementary File 2.

To score mRNAs as stress-resistant we used data from three independent studies where Integrated Stress Response was triggered in HEK293 cells either with arsenite (26,66) or tunicamycin (30). Translation efficiency for all transcripts was calculated using control and treatment conditions (data obtained in DDX3 knockout cell line from (66) were excluded) by normalizing the number of ribosome footprints aligning to CDS region over the average RNA-seq density and CDS length. Differential translation was measured upon Z-score transformation as in our earlier studies (22,26). Specifically transcripts were grouped into bins of 300 based on similarity of their expression levels and Z-scores were computed for each transcript based on log-fold changes of their translational efficiency between two conditions. These Z-scores were used as a measure of translational response to stress. The correlation was measured between Z-scores and each of the three features of uORFs, length, translation efficiency and pause scores (shown in Fig. 7). Pause scores were calculated using the same pooled data as those used for the detection of uORFs (26,30,61,66,73-79) by dividing the highest ribosome density at a single uORF location by the average ribosome footprint density of the corresponding uORF (excluding the highest peak coordinate).

ACKNOWLEDGMENTS.

This work was supported by Science Foundation Ireland grant (12/IA/1335) to PVB and Russian Science Foundation grant (RSF16-14-10065) to DEA. DR acknowledges the support of NSF through grant DMS-1413223. SJK and AMM wish to acknowledge individual support from Irish Research Council.

References

1. Hinnebusch, A.G., Ivanov, I.P. and Sonenberg, N. (2016) Translational control by 5'-untranslated regions of eukaryotic mRNAs. *Science*, **352**, 1413-1416.
2. Hinnebusch, A.G. (2014) The scanning mechanism of eukaryotic translation initiation. *Annu Rev Biochem*, **83**, 779-812.
3. Asano, K. (2014) Why is start codon selection so precise in eukaryotes? *Translation (Austin)*, **2**, e28387.
4. Topisirovic, I., Svitkin, Y.V., Sonenberg, N. and Shatkin, A.J. (2011) Cap and cap-binding proteins in the control of gene expression. *Wiley Interdiscip Rev RNA*, **2**, 277-298.
5. Jackson, R.J., Hellen, C.U. and Pestova, T.V. (2010) The mechanism of eukaryotic translation initiation and principles of its regulation. *Nat Rev Mol Cell Biol*, **11**, 113-127.
6. Pueyo, J.I., Magny, E.G. and Couso, J.P. (2016) New Peptides Under the s(ORF)ace of the Genome. *Trends Biochem Sci*, **41**, 665-678.
7. Johnstone, T.G., Bazzini, A.A. and Giraldez, A.J. (2016) Upstream ORFs are prevalent translational repressors in vertebrates. *EMBO J*, **35**, 706-723.
8. Wethmar, K. (2014) The regulatory potential of upstream open reading frames in eukaryotic gene expression. *Wiley Interdiscip Rev RNA*, **5**, 765-778.
9. von Arnim, A.G., Jia, Q. and Vaughn, J.N. (2014) Regulation of plant translation by upstream open reading frames. *Plant Sci*, **214**, 1-12.
10. Barbosa, C., Peixeiro, I. and Romao, L. (2013) Gene expression regulation by upstream open reading frames and human disease. *PLoS Genet*, **9**, e1003529.
11. Somers, J., Poyry, T. and Willis, A.E. (2013) A perspective on mammalian upstream open reading frame function. *Int J Biochem Cell Biol*, **45**, 1690-1700.
12. Vilela, C. and McCarthy, J.E. (2003) Regulation of fungal gene expression via short open reading frames in the mRNA 5' untranslated region. *Mol Microbiol*, **49**, 859-867.
13. Churbanov, A., Rogozin, I.B., Babenko, V.N., Ali, H. and Koonin, E.V. (2005) Evolutionary conservation suggests a regulatory function of AUG triplets in 5'-UTRs of eukaryotic genes. *Nucleic Acids Res*, **33**, 5512-5520.
14. Ivanov, I.P., Firth, A.E., Michel, A.M., Atkins, J.F. and Baranov, P.V. (2011) Identification of evolutionarily conserved non-AUG-initiated N-terminal extensions in human coding sequences. *Nucleic Acids Res*, **39**, 4220-4234.
15. Ivanov, I.P., Loughran, G. and Atkins, J.F. (2008) uORFs with unusual translational start codons autoregulate expression of eukaryotic ornithine decarboxylase homologs. *Proc Natl Acad Sci U S A*, **105**, 10079-10084.
16. Peabody, D.S. (1989) Translation initiation at non-AUG triplets in mammalian cells. *J Biol Chem*, **264**, 5031-5035.
17. Tzani, I., Ivanov, I.P., Andreev, D.E., Dmitriev, R.I., Dean, K.A., Baranov, P.V., Atkins, J.F. and Loughran, G. (2016) Systematic analysis of the PTEN 5' leader identifies a major AUU initiated proteoform. *Open Biol*, **6**.
18. Michel, A.M., Andreev, D.E. and Baranov, P.V. (2014) Computational approach for calculating the probability of eukaryotic translation initiation from ribo-seq data that takes into account leaky scanning. *BMC Bioinformatics*, **15**, 380.
19. Fritsch, C., Herrmann, A., Nothnagel, M., Szafranski, K., Huse, K., Schumann, F., Schreiber, S., Platzer, M., Krawczak, M., Hampe, J. et al. (2012) Genome-wide search for novel human uORFs and N-terminal protein extensions using ribosomal footprinting. *Genome Res*, **22**, 2208-2218.
20. Ingolia, N.T., Lareau, L.F. and Weissman, J.S. (2011) Ribosome profiling of mouse embryonic stem cells reveals the complexity and dynamics of mammalian proteomes. *Cell*, **147**, 789-802.

- 545 21. Lee, S., Liu, B., Lee, S., Huang, S.X., Shen, B. and Qian, S.B. (2012) Global mapping of translation
546 initiation sites in mammalian cells at single-nucleotide resolution. *Proc Natl Acad Sci U S A*, **109**,
547 E2424-2432.
- 548 22. Andreev, D.E., O'Connor, P.B., Zhdanov, A.V., Dmitriev, R.I., Shatsky, I.N., Papkovsky, D.B. and
549 Baranov, P.V. (2015) Oxygen and glucose deprivation induces widespread alterations in mRNA
550 translation within 20 minutes. *Genome Biol*, **16**, 90.
- 551 23. Shalgi, R., Hurt, J.A., Krykbaeva, I., Taipale, M., Lindquist, S. and Burge, C.B. (2013) Widespread
552 regulation of translation by elongation pausing in heat shock. *Mol Cell*, **49**, 439-452.
- 553 24. Gerashchenko, M.V., Lobanov, A.V. and Gladyshev, V.N. (2012) Genome-wide ribosome profiling
554 reveals complex translational regulation in response to oxidative stress. *Proc Natl Acad Sci U S A*,
555 **109**, 17394-17399.
- 556 25. Ingolia, N.T., Ghaemmaghami, S., Newman, J.R. and Weissman, J.S. (2009) Genome-wide
557 analysis in vivo of translation with nucleotide resolution using ribosome profiling. *Science*, **324**,
558 218-223.
- 559 26. Andreev, D.E., O'Connor, P.B., Fahey, C., Kenny, E.M., Terenin, I.M., Dmitriev, S.E., Cormican, P.,
560 Morris, D.W., Shatsky, I.N. and Baranov, P.V. (2015) Translation of 5' leaders is pervasive in
561 genes resistant to eIF2 repression. *Elife*, **4**, e03971.
- 562 27. Starck, S.R., Tsai, J.C., Chen, K., Shodiya, M., Wang, L., Yahiro, K., Martins-Green, M., Shastri, N.
563 and Walter, P. (2016) Translation from the 5' untranslated region shapes the integrated stress
564 response. *Science*, **351**, aad3867.
- 565 28. Young, S.K. and Wek, R.C. (2016) Upstream Open Reading Frames Differentially Regulate Gene-
566 specific Translation in the Integrated Stress Response. *J Biol Chem*, **291**, 16927-16935.
- 567 29. Baird, T.D. and Wek, R.C. (2012) Eukaryotic initiation factor 2 phosphorylation and translational
568 control in metabolism. *Adv Nutr*, **3**, 307-321.
- 569 30. Sidrauski, C., McGeachy, A.M., Ingolia, N.T. and Walter, P. (2015) The small molecule ISRIB
570 reverses the effects of eIF2alpha phosphorylation on translation and stress granule assembly.
571 *Elife*, **4**.
- 572 31. Hinnebusch, A.G. (1993) Gene-specific translational control of the yeast GCN4 gene by
573 phosphorylation of eukaryotic initiation factor 2. *Mol Microbiol*, **10**, 215-223.
- 574 32. Gunisova, S., Beznoskova, P., Mohammad, M.P., Vlckova, V. and Valasek, L.S. (2016) In-depth
575 analysis of cis-determinants that either promote or inhibit reinitiation on GCN4 mRNA after
576 translation of its four short uORFs. *RNA*, **22**, 542-558.
- 577 33. Gunisova, S. and Valasek, L.S. (2014) Fail-safe mechanism of GCN4 translational control--uORF2
578 promotes reinitiation by analogous mechanism to uORF1 and thus secures its key role in GCN4
579 expression. *Nucleic Acids Res*, **42**, 5880-5893.
- 580 34. Dever, T.E., Feng, L., Wek, R.C., Cigan, A.M., Donahue, T.F. and Hinnebusch, A.G. (1992)
581 Phosphorylation of initiation factor 2 alpha by protein kinase GCN2 mediates gene-specific
582 translational control of GCN4 in yeast. *Cell*, **68**, 585-596.
- 583 35. Palam, L.R., Baird, T.D. and Wek, R.C. (2011) Phosphorylation of eIF2 facilitates ribosomal bypass
584 of an inhibitory upstream ORF to enhance CHOP translation. *J Biol Chem*, **286**, 10939-10949.
- 585 36. Chen, Y.J., Tan, B.C., Cheng, Y.Y., Chen, J.S. and Lee, S.C. (2010) Differential regulation of CHOP
586 translation by phosphorylated eIF4E under stress conditions. *Nucleic Acids Res*, **38**, 764-777.
- 587 37. Lee, Y.Y., Cevallos, R.C. and Jan, E. (2009) An upstream open reading frame regulates translation
588 of GADD34 during cellular stresses that induce eIF2alpha phosphorylation. *J Biol Chem*, **284**,
589 6661-6673.
- 590 38. Zach, L., Braunstein, I. and Stanhill, A. (2014) Stress-induced start codon fidelity regulates
591 arsenite-inducible regulatory particle-associated protein (AIRAP) translation. *J Biol Chem*, **289**,
592 20706-20716.
- 593 39. Young, S.K., Palam, L.R., Wu, C., Sachs, M.S. and Wek, R.C. (2016) Ribosome Elongation Stall
594 Directs Gene-specific Translation in the Integrated Stress Response. *J Biol Chem*, **291**, 6546-
595 6558.

- 596 40. Ciandrini, L., Stansfield, I. and Romano, M.C. (2010) Role of the particle's stepping cycle in an
597 asymmetric exclusion process: a model of mRNA translation. *Phys Rev E Stat Nonlin Soft Matter*
598 *Phys*, **81**, 051904.
- 599 41. Margaliot, M. and Tuller, T. (2012) Stability analysis of the ribosome flow model. *IEEE/ACM*
600 *Trans Comput Biol Bioinform*, **9**, 1545-1552.
- 601 42. Reuveni, S., Meilijson, I., Kupiec, M., Ruppín, E. and Tuller, T. (2011) Genome-scale analysis of
602 translation elongation with a ribosome flow model. *PLoS Comput Biol*, **7**, e1002127.
- 603 43. von der Haar, T. (2012) Mathematical and Computational Modelling of Ribosomal Movement
604 and Protein Synthesis: an overview. *Comput Struct Biotechnol J*, **1**, e201204002.
- 605 44. Zhao, Y.B. and Krishnan, J. (2014) mRNA translation and protein synthesis: an analysis of
606 different modelling methodologies and a new PBN based approach. *BMC Syst Biol*, **8**, 25.
- 607 45. Zia, R., Dong, J. and Schmittmann, B. (2011) Modeling translation in protein synthesis with
608 TASEP: A tutorial and recent developments. *arXiv preprint arXiv:1108.3312*.
- 609 46. Wolin, S.L. and Walter, P. (1988) Ribosome pausing and stacking during translation of a
610 eukaryotic mRNA. *EMBO J*, **7**, 3559-3569.
- 611 47. Steitz, J.A. (1969) Polypeptide chain initiation: nucleotide sequences of the three ribosomal
612 binding sites in bacteriophage R17 RNA. *Nature*, **224**, 957-964.
- 613 48. Archer, S.K., Shirokikh, N.E., Beilharz, T.H. and Preiss, T. (2016) Dynamics of ribosome scanning
614 and recycling revealed by translation complex profiling. *Nature*, **535**, 570-574.
- 615 49. Ivanov, I.P., Shin, B.S., Loughran, G., Tzani, I., Young-Baird, S.K., Cao, C., Atkins, J.F. and Dever,
616 T.E. (2018) Polyamine Control of Translation Elongation Regulates Start Site Selection on
617 Antizyme Inhibitor mRNA via Ribosome Queuing. *Mol Cell*, **70**, 254-264 e256.
- 618 50. Vassilenko, K.S., Alekhina, O.M., Dmitriev, S.E., Shatsky, I.N. and Spirin, A.S. (2011)
619 Unidirectional constant rate motion of the ribosomal scanning particle during eukaryotic
620 translation initiation. *Nucleic Acids Res*, **39**, 5555-5567.
- 621 51. Berthelot, K., Muldoon, M., Rajkowitsch, L., Hughes, J. and McCarthy, J.E. (2004) Dynamics and
622 processivity of 40S ribosome scanning on mRNA in yeast. *Mol Microbiol*, **51**, 987-1001.
- 623 52. Chu, D., Kazana, E., Bellanger, N., Singh, T., Tuite, M.F. and von der Haar, T. (2014) Translation
624 elongation can control translation initiation on eukaryotic mRNAs. *EMBO J*, **33**, 21-34.
- 625 53. Shah, P., Ding, Y., Niemczyk, M., Kudla, G. and Plotkin, J.B. (2013) Rate-limiting steps in yeast
626 protein translation. *Cell*, **153**, 1589-1601.
- 627 54. Tuller, T., Waldman, Y.Y., Kupiec, M. and Ruppín, E. (2010) Translation efficiency is determined
628 by both codon bias and folding energy. *Proc Natl Acad Sci U S A*, **107**, 3645-3650.
- 629 55. Wen, J.D., Lancaster, L., Hodges, C., Zeri, A.C., Yoshimura, S.H., Noller, H.F., Bustamante, C. and
630 Tinoco, I. (2008) Following translation by single ribosomes one codon at a time. *Nature*, **452**,
631 598-603.
- 632 56. Kozak, M. (1999) Initiation of translation in prokaryotes and eukaryotes. *Gene*, **234**, 187-208.
- 633 57. Mohammad, M.P., Munzarova Pondelickova, V., Zeman, J., Gunisova, S. and Valasek, L.S. (2017)
634 In vivo evidence that eIF3 stays bound to ribosomes elongating and terminating on short
635 upstream ORFs to promote reinitiation. *Nucleic Acids Res*, **45**, 2658-2674.
- 636 58. Young, S.K., Willy, J.A., Wu, C., Sachs, M.S. and Wek, R.C. (2015) Ribosome Reinitiation Directs
637 Gene-specific Translation and Regulates the Integrated Stress Response. *J Biol Chem*, **290**,
638 28257-28271.
- 639 59. Valasek, L., Szamecz, B., Hinnebusch, A.G. and Nielsen, K.H. (2007) In vivo stabilization of
640 preinitiation complexes by formaldehyde cross-linking. *Methods Enzymol*, **429**, 163-183.
- 641 60. Dmitriev, S.E., Andreev, D.E., Terenin, I.M., Olovnikov, I.A., Prassolov, V.S., Merrick, W.C. and
642 Shatsky, I.N. (2007) Efficient translation initiation directed by the 900-nucleotide-long and GC-
643 rich 5' untranslated region of the human retrotransposon LINE-1 mRNA is strictly cap dependent
644 rather than internal ribosome entry site mediated. *Mol Cell Biol*, **27**, 4685-4697.
- 645 61. Guo, J.U., Agarwal, V., Guo, H. and Bartel, D.P. (2014) Expanded identification and
646 characterization of mammalian circular RNAs. *Genome Biol*, **15**, 409.

62. Oh, E., Becker, A.H., Sandikci, A., Huber, D., Chaba, R., Gloge, F., Nichols, R.J., Typas, A., Gross, C.A., Kramer, G. *et al.* (2011) Selective ribosome profiling reveals the cotranslational chaperone action of trigger factor in vivo. *Cell*, **147**, 1295-1308.
63. Sin, C., Chiarugi, D. and Valleriani, A. (2016) Quantitative assessment of ribosome drop-off in *E. coli*. *Nucleic Acids Res*, **44**, 2528-2537.
64. Lareau, L.F., Hite, D.H., Hogan, G.J. and Brown, P.O. (2014) Distinct stages of the translation elongation cycle revealed by sequencing ribosome-protected mRNA fragments. *Elife*, **3**, e01257.
65. Pisarev, A.V., Kolupaeva, V.G., Yusupov, M.M., Hellen, C.U. and Pestova, T.V. (2008) Ribosomal position and contacts of mRNA in eukaryotic translation initiation complexes. *EMBO J*, **27**, 1609-1621.
66. Oh, S., Flynn, R.A., Floor, S.N., Purzner, J., Martin, L., Do, B.T., Schubert, S., Vaka, D., Morrissy, S., Li, Y. *et al.* (2016) Medulloblastoma-associated DDX3 variant selectively alters the translational response to stress. *Oncotarget*, **7**, 28169-28182.
67. Michel, A.M., Fox, G., A, M.K., De Bo, C., O'Connor, P.B., Heaphy, S.M., Mullan, J.P., Donohue, C.A., Higgins, D.G. and Baranov, P.V. (2014) GWIPS-viz: development of a ribo-seq genome browser. *Nucleic Acids Res*, **42**, D859-864.
68. Michel, A.M., Kiniry, S.J., O'Connor, P.B.F., Mullan, J.P. and Baranov, P.V. (2018) GWIPS-viz: 2018 update. *Nucleic Acids Res*, **46**, D823-D830.
69. O'Connor, P.B., Andreev, D.E. and Baranov, P.V. (2016) Comparative survey of the relative impact of mRNA features on local ribosome profiling read density. *Nat Commun*, **7**, 12915.
70. Leprivier, G., Remke, M., Rotblat, B., Dubuc, A., Mateo, A.R., Kool, M., Agnihotri, S., El-Naggar, A., Yu, B., Somasekharan, S.P. *et al.* (2013) The eEF2 kinase confers resistance to nutrient deprivation by blocking translation elongation. *Cell*, **153**, 1064-1079.
71. Zinshteyn, B., Rojas-Duran, M.F. and Gilbert, W.V. (2017) Translation initiation factor eIF4G1 preferentially binds yeast transcript leaders containing conserved oligo-uridine motifs. *RNA*, **23**, 1365-1375.
72. Arnold, M. (2018) uORF_TASEP_ICIER. *GitHub*, https://github.com/maximarnold/uORF_TASEP_ICIER, 118d650.
73. Park, Y., Reyna-Neyra, A., Philippe, L. and Thoreen, C.C. (2017) mTORC1 Balances Cellular Amino Acid Supply with Demand for Protein Synthesis through Post-transcriptional Control of ATF4. *Cell Rep*, **19**, 1083-1090.
74. Lintner, N.G., McClure, K.F., Petersen, D., Londregan, A.T., Piotrowski, D.W., Wei, L., Xiao, J., Bolt, M., Loria, P.M., Maguire, B. *et al.* (2017) Selective stalling of human translation through small-molecule engagement of the ribosome nascent chain. *PLoS Biol*, **15**, e2001882.
75. Park, J.E., Yi, H., Kim, Y., Chang, H. and Kim, V.N. (2016) Regulation of Poly(A) Tail and Translation during the Somatic Cell Cycle. *Mol Cell*, **62**, 462-471.
76. Xu, B., Gogol, M., Gaudenz, K. and Gerton, J.L. (2016) Improved transcription and translation with L-leucine stimulation of mTORC1 in Roberts syndrome. *BMC Genomics*, **17**, 25.
77. Calviello, L., Mukherjee, N., Wyler, E., Zaubler, H., Hirsekorn, A., Selbach, M., Landthaler, M., Obermayer, B. and Ohler, U. (2016) Detecting actively translated open reading frames in ribosome profiling data. *Nat Methods*, **13**, 165-170.
78. Tirosh, O., Cohen, Y., Shitrit, A., Shani, O., Le-Trilling, V.T., Trilling, M., Friedlander, G., Tanenbaum, M. and Stern-Ginossar, N. (2015) The Transcription and Translation Landscapes during Human Cytomegalovirus Infection Reveal Novel Host-Pathogen Interactions. *PLoS Pathog*, **11**, e1005288.
79. Werner, A., Iwasaki, S., McGourty, C.A., Medina-Ruiz, S., Teerikorpi, N., Fedrigo, I., Ingolia, N.T. and Rape, M. (2015) Cell-fate determination by ubiquitin-dependent regulation of translation. *Nature*, **525**, 523-527.
80. Rodriguez, J.M., Maietta, P., Ezkurdia, I., Pietrelli, A., Wesselink, J.J., Lopez, G., Valencia, A. and Tress, M.L. (2013) APPRIS: annotation of principal and alternative splice isoforms. *Nucleic acids research*, **41**, D110-117.